

Supporting Information for

Gate-Tunable Plasmon-Enhanced Photodetection in a Monolayer MoS₂

Phototransistor with Ultrahigh Photoresponsivity

Hao-Yu Lan,¹ Yu-Hung Hsieh,^{1,2} Zong-Yi Chiao,^{1,3} Deep Jariwala,⁴ Min-Hsiung Shih,¹ Ta-Jen Yen,²
Ortwin Hess,^{5,6} and Yu-Jung Lu^{*1,3}

¹*Research Center for Applied Sciences, Academia Sinica, Taipei 11529, Taiwan*

²*Department of Materials Science and Engineering, National Tsing Hua University, Hsinchu 30013, Taiwan*

³*Department of Physics, National Taiwan University, Taipei 10617, Taiwan*

⁴*Department of Electrical and Systems Engineering, University of Pennsylvania, Philadelphia, PA, USA*

⁵*Blackett Laboratory, Imperial College London, South Kensington Campus, SW7 2AZ London, United Kingdom*

⁶*School of Physics and CRANN Institute, Trinity College Dublin, Dublin 2, Ireland*

*To whom correspondence should be addressed.

E-mail: yujunglu@gate.sinica.edu.tw

Table of contents

Section S1. Gold-mediated exfoliation

Section S2. Raman and PL spectra of the monolayer MoS₂

Section S3. The measured optical constants of noble metal (Au, Ag, Al) films

Section S4. Full-Color palettes with varied size and period of Ag nanodisk arrays

Section S5. Reflection spectra of different Ag nanodisk arrays with varied disk size and period

Section S6. Calculated absorption spectra specifically for the monolayer MoS₂ layer

Section S7. Metrics of the reported TMD-based plasmonic photodetectors

Section S1. Gold-mediated exfoliation

Monolayer MoS₂ was prepared by a gold-mediated exfoliation method¹. This advanced method starts with gold (Au) evaporation (~ 100 nm) on bulk MoS₂. The interaction between Au and S atoms on the topmost layer is much stronger than that between the same layer and the bottom layer, thus enabling peel-off of the topmost layer by using thermal tape. The thermal tape is then released on a hot plate (=120°C) and cleaned by O₂ plasma treatment. The top Au film is etched by potassium iodide and iodine (KI/I₂) wet etching, followed by a 10 min acetone and isopropyl alcohol (IPA) rinse to remove the etchant and the residues.

Section S2. Raman and PL spectra of the monolayer MoS₂

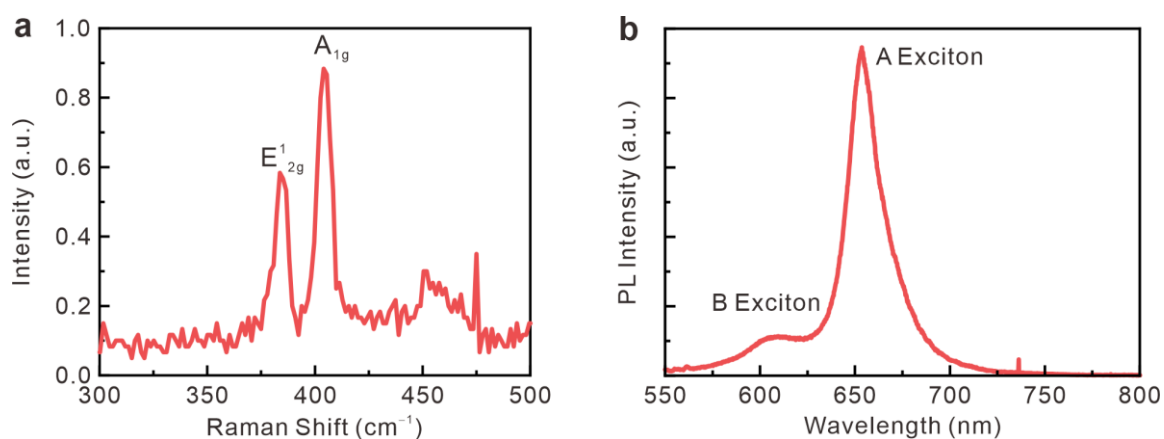


Figure S1. Material properties of monolayer MoS₂ obtained by gold-mediated exfoliation method. (a) Raman spectra and (b) photoluminescence (PL) spectra of monolayer MoS₂.

Section S3. The measured optical constants of noble metal (Au, Ag, Al) films

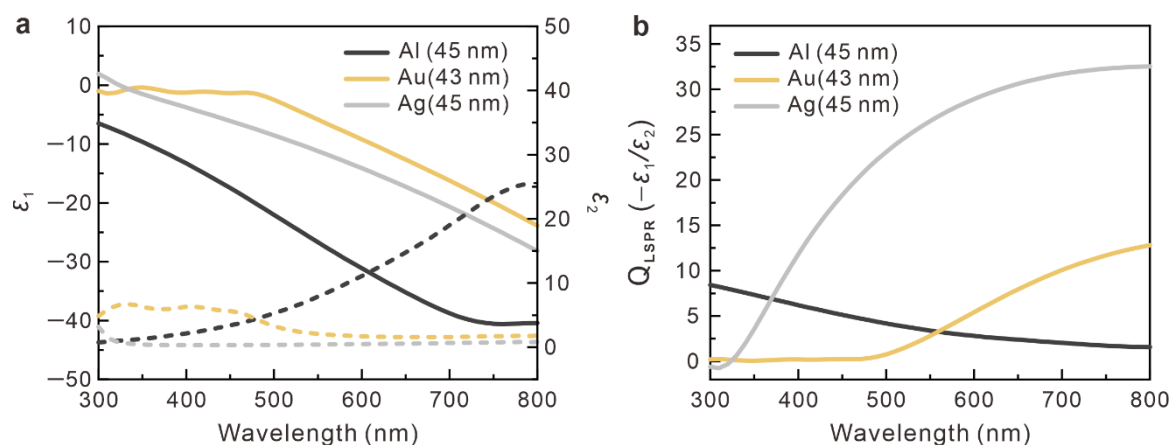


Figure S2. The measured optical constants of noble metal (Au, Ag, Al) films growth by thermal evaporation. The base pressure of the vacuum chamber is approximately 3×10^{-6} torr, and the deposition rate is approximately 1 \AA s^{-1} . (a) The optical constants of Al, Au, and Ag were measured by spectroscopic ellipsometry (VASE, J.A. Woollam Co.). The real (solid line) and imaginary (dashed line) parts of the dielectric function are used for the FDTD simulation. (b) Calculated quality factors of the localized surface plasmon resonance in spherical structures (Q_{LSPR}). The results suggest that Ag is the best plasmonic material in the visible.

Section S4. Full-Color palettes with varied size and period of plasmonic Ag nanodisk arrays

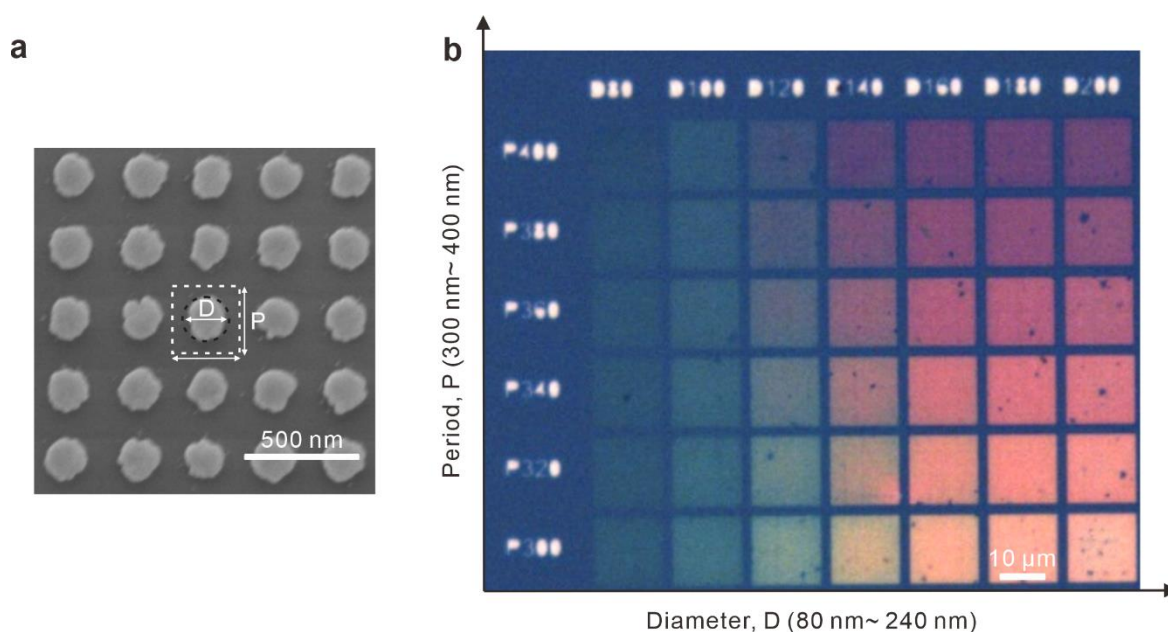


Figure S3. Full-color palettes with varied size and period of plasmonic Ag nanodisk (ND) arrays on SiO₂/Si substrate. (a) SEM images of a fabricated AgND array with a diameter of 140 nm and a periodicity of 260 nm. (b) Optical image of the reflective colors from different AgND arrays with the designed disk size D= 80– 240 nm) and the designed period P= 220– 400 nm. The real size of the fabricated AgNDs is slightly larger than the designed size. The image was taken using a 20 \times objective lens in microscope reflection mode under a white light illumination.

Section S5. Reflection spectra of different Ag nanodisk arrays with varied disk size and period

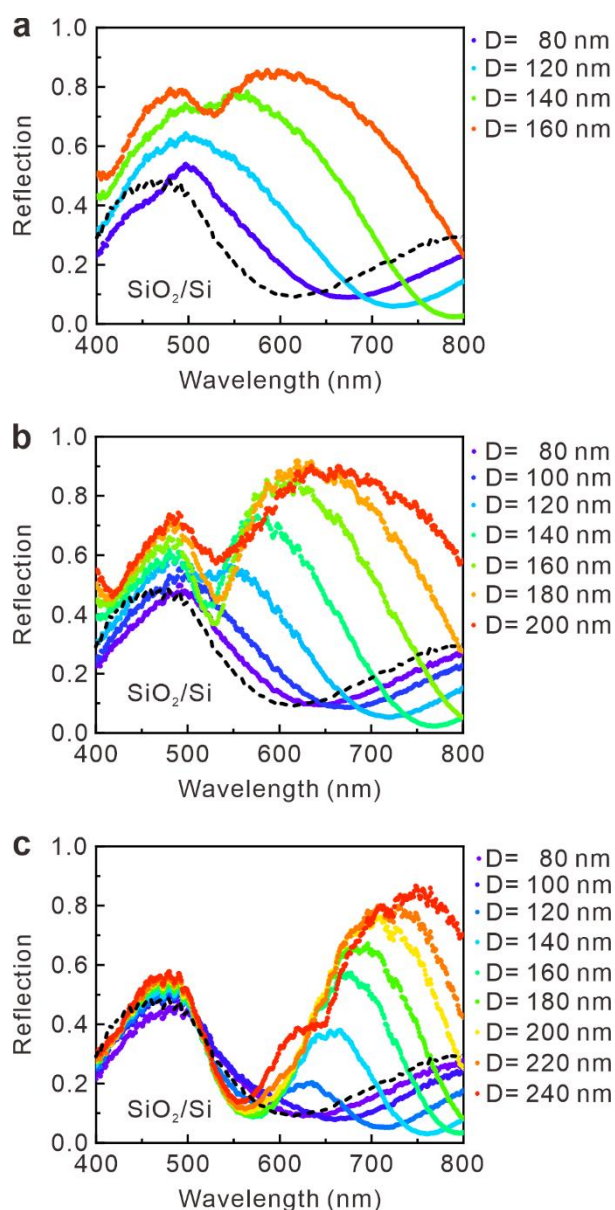


Figure S4. Measured reflection spectra of different Ag nanodisk (AgND) arrays with varied disk size and period on the SiO_2/Si substrate. (a) Experimentally measured reflection spectra from AgND arrays with a varied diameter of the AgND at a fixed period of $P = 260$ nm. (b) $P = 300$ nm. (c) $P = 400$ nm. The black line shows the reflection spectra from the SiO_2/Si substrate. A clear redshift in the resonance peak with increasing diameter of AgND is strongly related to the localized surface plasmon resonance in the AgND arrays.

Section S6. Calculated absorption spectra specifically for the monolayer MoS₂ layer

The simulation results of the monolayer MoS₂ absorbance were done with the commercial Lumerical FDTD software. In the simulation setup, a 300 nm silica layer was located on the silicon substrate. On top of the silica, the monolayer MoS₂ with a thickness of 0.7 nm was then defined. The permittivity of the monolayer MoS₂ was taken from the literature². In the case of plasmonic enhancement, the silver nanodisk (diameter = 160 nm, height = 40 nm) was built on the monolayer MoS₂. To construct the nanodisk arrays, periodic boundary conditions (period = 260 nm) were set in the x and y directions, while the PML boundaries were applied in the z direction, with a planewave source propagating in the same direction. The mesh for each simulation was set to be 1 nm in the x and y directions and 0.2 nm in the z direction. To obtain the absorbance of the monolayer MoS₂, a field monitor and an index monitor were added to cover the entire region of the MoS₂ layer. The absorbance was then calculated by applying equation (1) and integrating through the volume of the MoS₂ monolayer.

$$Absorbance = \frac{1}{2} \times \varepsilon_0 \times \omega \times |E|^2 \times \varepsilon_{img} \quad (1)$$

where ε_0 , ω , E , and ε_{img} represent the permittivity of free space, the angular frequency, the normalized electric field (by the source), and the imaginary part of epsilon of the monolayer MoS₂, respectively.

Section S7. Metrics of the reported TMD-based plasmonic photodetectors

Devices	Material	Plasmonic Structure	Responsivity (A W ⁻¹)	Detectivity (cm Hz ^{1/2} W ⁻¹)	Decay Time (s)	Enhanced Ratio
PhotoFET	FL MoS ₂	Au nanoparticles (SHINs) ³	NA	NA	NA	2-3
	1L MoS ₂	Au nanoshells ⁴	~0.87 mA W ⁻¹ @630 nm	NA	NA	1.5-3.5
	FL MoS ₂	Au nanoparticles ⁵	~ 2-3 mA W ⁻¹ @632 nm	NA	NA	2
	FL MoS ₂	Au nanoarrays ⁵	~ 2-3 mA W ⁻¹ @632 nm	NA	NA	3
	FL MoS ₂	Au nanoarrays ⁶	20 A W ⁻¹ @ 466 nm	6×10^{10}	0.58 s	8.2
	1L MoS₂	Ag nanoarrays (This work)	~27000 A/W @ 620 nm	1.3×10^{12}	0.4 s	7.2
M-S-M PD	1L MoS ₂	Ag nanowires ⁷	59.6 A/W @532 nm	4.51×10^{10}	> 10 s	250
	1L MoS ₂	Ag nanoparticles (SHINs) ⁸	287.5 A/W @570 nm	NA	15 s	8.8
	1L MoS ₂	Ag nanocubes ⁹	7940 A/W @520 nm	NA	1.6 s	38
	FL MoS ₂	Au nanoparticles ¹⁰	64 mA/W @980 nm	NA	2.6 ms	14

Table S1. Device performance of the reported plasmonic-enhanced monolayer or multi-layer MoS₂ photodetectors.

References

- (1) Desai, S. B.; Madhvapathy, S. R.; Amani, M.; Kiriya, D.; Hettick, M.; Tosun, M.; Zhou, Y.; Dubey, M.; Ager, J. W., 3rd; Chrzan, D.; Javey, A., Gold-mediated exfoliation of ultralarge optoelectronically-perfect monolayers. *Adv. Mater.* **2016**, *28*, (21), 4053–4058.
- (2) Bablu Mukherjee, F. T., Daniel Gunlycke, Kiran Kumar Amara, Goki Eda, and Ergun Simsek, Complex electrical permittivity of the monolayer molybdenum disulfide (MoS_2) in near UV and visible. *Opt. Mater. Express* **2015**, *5*, (2), 447–455.
- (3) Lin, J.; Li, H.; Zhang, H.; Chen, W., Plasmonic enhancement of photocurrent in MoS_2 field-effect-transistor. *Appl. Phys. Lett.* **2013**, *102*, (20), 203109.
- (4) Sobhani, A.; Lauchner, A.; Najmaei, S.; Ayala-Orozco, C.; Wen, F.; Lou, J.; Halas, N. J., Enhancing the photocurrent and photoluminescence of single crystal monolayer MoS_2 with resonant plasmonic nanoshells. *Appl. Phys. Lett.* **2014**, *104*, (3), 031112.
- (5) Miao, J.; Hu, W.; Jing, Y.; Luo, W.; Liao, L.; Pan, A.; Wu, S.; Cheng, J.; Chen, X.; Lu, W., Surface plasmon-enhanced photodetection in few layer MoS_2 phototransistors with Au nanostructure arrays. *Small* **2015**, *11*, (20), 2392–2398.
- (6) Lee, S.; Park, J.; Yun, Y.; Lee, J.; Heo, J., Enhanced photoresponsivity of multilayer MoS_2 phototransistor using localized Au schottky junction formed by spherical-lens photolithography. *Adv. Mater. Interfaces* **2019**, *6*, (8), 1900053.
- (7) Bang, S.; Duong, N. T.; Lee, J.; Cho, Y. H.; Oh, H. M.; Kim, H.; Yun, S. J.; Park, C.; Kwon, M. K.; Kim, J. Y.; Kim, J.; Jeong, M. S., Augmented quantum yield of a 2D monolayer photodetector by surface plasmon coupling. *Nano Lett.* **2018**, *18*, (4), 2316–2323.
- (8) Wu, Z. Q.; Yang, J. L.; Manjunath, N. K.; Zhang, Y. J.; Feng, S. R.; Lu, Y. H.; Wu, J. H.; Zhao, W. W.; Qiu, C. Y.; Li, J. F.; Lin, S. S., Gap-mode surface-plasmon-enhanced photoluminescence and photoresponse of MoS_2 . *Adv. Mater.* **2018**, *30*, (27), e1706527.
- (9) Sun, B.; Wang, Z.; Liu, Z.; Tan, X.; Liu, X.; Shi, T.; Zhou, J.; Liao, G., Tailoring of silver nanocubes with optimized localized surface plasmon in a gap mode for a flexible MoS_2 photodetector. *Adv. Funct. Mater.* **2019**, *29*, (26), 1900541.
- (10) Guo, J.; Li, S.; He, Z.; Li, Y.; Lei, Z.; Liu, Y.; Huang, W.; Gong, T.; Ai, Q.; Mao, L.; He, Y.; Ke, Y.; Zhou, S.; Yu, B., Near-infrared photodetector based on few-layer MoS_2 with sensitivity enhanced by localized surface plasmon resonance. *Appl. Surf. Sci.* **2019**, *483*, 1037–1043.